Desalination and Water Treatment
www.deswater.com
doi: 10.1080/19443994.2014.982962

56 (2015) 2754–2765
December

Taylor & Francis
Taylor & Francis Group

Removal of toluidine blue from aqueous solution using orange peel waste (OPW)

Ridha Lafi, Souad Rezma, Amor Hafiane*

Laboratory of Wastewater Treatment, CERTE BP 273, 8020 Soliman, Tunisia, email: amor.hafiane@certe.rnrt.tn (A. Hafiane)

Received 22 November 2013; Accepted 22 October 2014

ABSTRACT

The adsorption of toluidine blue, a basic dye, onto orange peel waste (OPW) was investigated using a batch adsorption technique. A series of assays were undertaken to assess the effect of the system variables, i.e. initial dye concentration, amount of adsorbent, pH, ionic strength, and solution temperature. The experimental data were analyzed by Langmuir, Freundlich, and Temkin isotherm models. Equilibrium data fitted well with the Langmuir model with maximum monolayer adsorption capacity of 314.3 mg g^{-1}. Besides, the experimental results showed that the pseudo-second-order equation is the best model that describes the adsorption behavior and rate constants were estimated. Thermodynamic parameters were evaluated and the negative value of ΔH indicated exothermic nature of adsorption. This work demonstrates that OPW is suitable as an adsorbent material for adsorption from aqueous solutions.

Keywords: Adsorption; Orange peel waste; Toluidine blue; Isotherms; Kinetics

1. Introduction

Industries such as textile, leather, paper, paint, plastics, etc, use dyes in order to color their products and also consumed substantial volumes of water [1]. As a result, they generate a considerable amount of colored wastewater. Today, there are more than 10,000 dyes with different chemical structures available commercially. Among these dyes, many are toxic and have carcinogenic and mutagenic effects [2]. So, the colored effluents have to be treated before they are discharged into the water bodies. Techniques such as anaerobic/aerobic treatment [3], coagulation/flocculation [4], oxidation/ozonation [5], membrane separation [6], and adsorption [7] have been tested and evaluated for the treatment of dye bearing effluents. Among them, adsorption process is one of the effective techniques that have been successfully employed for color removal from wastewater [8]. In this connection, many natural adsorbents such as garlic peel [9], grapefruit peel [10], wood apple shell [11], and orange waste [12] have been tested to reduce dye concentrations from aqueous solutions.

Citrus fruits which are abundant in Tunisia, mainly in the Cap Bon region, the annual production reached 330,000 tons (INS, 2012 statistic). The "Maltaise" variety is the most representative of the produced oranges among several varieties cultivated in Tunisia (DGPA,

*Corresponding author.

Presented at the 4th Maghreb Conference on Desalination and Water Treatment (CMTDE 2013) 15–18 December 2013, Hammamet, Tunisia

2012) with consumption in the order of 260,000 tons (INS, 2008). After juice extraction the residual peel accounts for 50 wt.% of the fruit, presenting an environmental problem. Aside from some important uses from aromatize tea, cake, and sugars, all the quantities of orange peel end up in the form of waste in the discharges. The approximate chemical composition of the orange peel is very rich in fiber: 42.12, large amount of soluble sugars (g/100 g): 46.64, proteins (g/100 g): 8.01, and moisture (g/g): 2.97 [13]. Orange peel contains several water soluble, and insoluble monomers and polymers [14,15]. The water soluble fraction contains glucose, fructose, sucrose, and some xylose, while pectin, cellulose, hemicelluloses, and lignin constitute between 50 and 70% of the insoluble fraction. These polymers are rich in carboxyl and hydroxyl functional groups, which may bind cationic dye molecules in aqueous solution [16].

The aim of the present work was to evaluate the efficiency of the removal of toluidine blue (TB) from aqueous solutions using orange peel waste (OPW) as an adsorbent. TB chosen as model molecule is a basic dye which has been shown to have harmful effects on living organisms on short period of exposure. The effects of contact time, initial dye concentration, pH, ionic strength, and temperature of dye solution and adsorbent dose on the adsorption capacity were investigated to optimize the conditions leading to maximum removal efficiency. Moreover, kinetic and equilibrium models were used to fit the experimental data.

2. Experimental

2.1. Adsorbent

OPW used in this study was obtained from a juice shop in the center of Tunis (Tunisia). The peels were washed with distilled water several times to remove ash and other contaminants and then dried in an oven at 70˚C for 24 h. The dried OPW was crushed and sieved through AFNOR sieves of 250 μm size and used as such.

2.2. Adsorbate

TB, a basic dye, C·I. 52040, $\lambda_{max} = 623$ nm, molecular formula $C_{15}H_{16}ClN_3S$, was purchased from Fluka. The chemical structure of TB is shown in Fig. 1. A stock solution of 1.0 g L^{-1} was prepared by dissolving the appropriate amount of TB in 100 mL and completing to 1,000 mL with distilled water. pH adjustments have been done using solutions of 0.1 M HCl or 0.1 M NaOH.

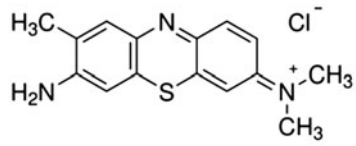

Fig. 1. Chemical structure of toluidine blue.

2.3. Characterization of orange peel waste

The specific surface area and pore structure parameters of adsorbent were determined from the adsorption–desorption isotherm of nitrogen using a Quantachrome instrument model Autosorb-1.

The surface structure of the OPW was explored with Fourier transform infrared spectroscopy (FTIR) to identify alterations on the adsorbent surface before and after dye adsorption (using a KBr disc technique in the range of 400–4,000 cm^{-1}).

Acidic and basic sites on waste orange peel were determined by the acid–base titration method proposed by Boehm [17]. The total acid sites were neutralized using 0.1 M NaOH while the basic sites were neutralized with 0.1 M HCl. The acidic and basic sites were determined by leaving 50 mL of 0.1 mol L^{-1} titration solutions and 1 g of OPW for 5 d at room temperature with occasional shaking, before titration a 10 mL sample of 0.1 M HCl or NaOH solution is added.

The point of zero charge (PZC) was determined by the solid addition methods [18]. To a series of 250 mL erlenmeyer flask; 50 mL of KNO_3 (0.1 M) was transferred. The initial pH of the solutions was adjusted to a value between 2 and 10 by adding 0.1 M HCl or NaOH solutions. Then, 0.1 g of OPW was added to each flask, stirred, and the final pH of the solutions was measured after 48 h. The value of PZC can be determined from the curve that cuts the pH_i line of the plot (pH_f–pH_i) vs. pH_i. The value of PZC is around 3.6 from aqueous solutions (Fig. 2).

2.4. Adsorption studies

Adsorption experiments were carried out by shaking a fixed 0.3 g of OPW with 100 ml of different initial dye solution (20–160 mg L^{-1}). Studies were conducted at 25 ± 1˚C using thermo-regulated water bath operating at 220 rpm. Samples were then centrifugated, and the left out concentration in the supernatant solution were analyzed using UV/VIS spectrometry.

The effect of pH on the removal of TB was evaluated in the pH range of 2.5–10.4 by addition of dilute

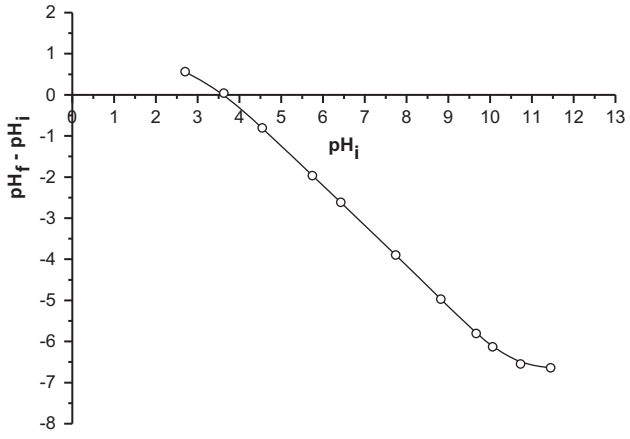

Fig. 2. PZC of OPW.

HCl or NaOH solutions. The effects of temperature on the adsorption data were carried out by performing the adsorption experiments at various temperatures (25, 35, 45, and 55°C).

The removal percentage of TB was measured and the percentage removal dye was calculated using the following equation:

$$\%\ \text{dye removal} = \frac{C_i - C_e}{C_i} \times 100 \quad (1)$$

where C_i (mg L^{-1}) and C_e (mg L^{-1}) are the initial and final concentrations of dye. The amount of dye adsorbed onto OPW q_e (mg g^{-1}) was calculated by the following relationship:

$$q_e = (C_i - C_e)\frac{V}{W} \quad (2)$$

where C_i and C_e (mg L^{-1}) are the initial and equilibrium dye concentrations in aqueous solution, respectively, V (L) is the volume of the solution, and W (g) is the weight of the adsorbent (g).

3. Results and discussion

3.1. Characterization of adsorbent

The results of PZC and Bohem titration of OPW are reported in Table 1. The BET surface area, total pore volume, and average pore diameter of the OPW were found to be 1.026 $m^2 g^{-1}$, 0.014 $cm^3 g^{-1}$, and 53.77 nm, respectively. We can see that OPW has very small surface area (<2 $m^2 g^{-1}$) but large pore sizes. According to the classification of IUPAC-pore dimensions the vast majority of the pores fall into the range

Table 1
PZC and Bohem titration of OPW

Biosorbent	OPW
PZC	3.6
Total acidic sites (mmol g^{-1})	2.15
Basic sites (mmol g)	0.25

of macropore ($d > 50$ nm). Macropores are not important for the adsorption capacity, but they act as transport pores to the mesopores and micropores [19]. Isotherm (N_2-adsorption/desorption) showed the presence of a hysteresis loop which indicated an isotherm type II and an adsorption hysteresis type H4 (Fig. 3). The distribution of pore size is not well-defined and can be associated with a combination of mesoporous–acroporous structure [20]. There was an increase in the adsorption capacity at a relative pressure higher than 0.1 and a sharp rise at a relative pressure higher than 0.8. The increase in the plateau in the range 0.2–0.8 indicated that the mesopore development had started [21].

FTIR spectra analyses for OPW before and after adsorption of TB were undertaken and results are shown in Fig. 4 and Table 2. OPW FTIR spectrum presents a broad and intense absorption bands observed from 3,000 to 3,600 cm^{-1} indicating the presence of free or hydrogen-bonded O–H groups (alcohols, phenols, and carboxylic acids) [22]. The O–H stretching vibrations occur within a broad range of frequencies indicating the presence of "free" hydroxyl groups and

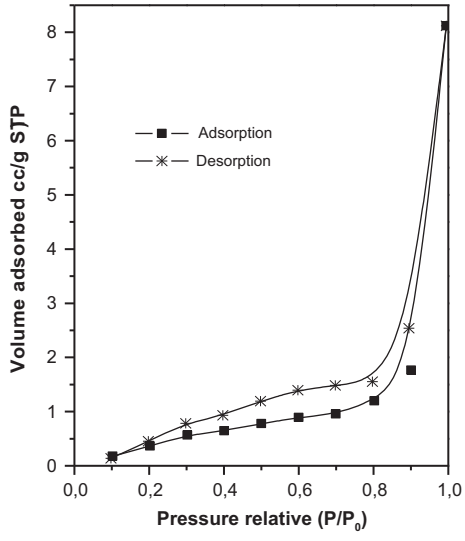

Fig. 3. N_2 adsorption−desorption isotherm of OPW.

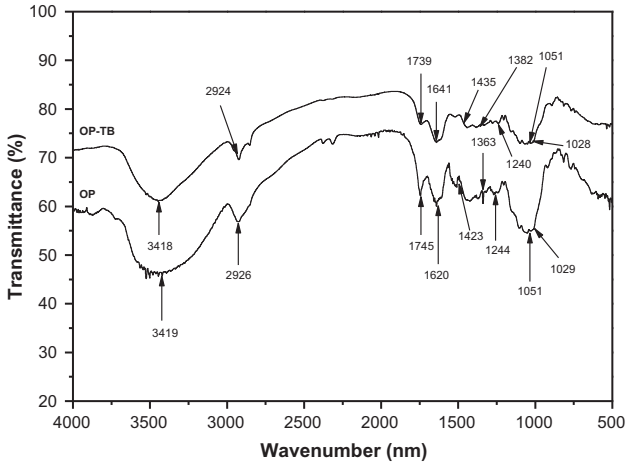

Fig. 4. FTIR of spectra of OPW and OPW-TB.

bonded O–H bands of carboxylic acids. The absorption band observed at 2,926 cm^{-1} is attributed to the C–H bonds of aliphatic acids [23]. A band at 1,739 cm^{-1} is related with the C=O stretching bond of non-ionic carboxyl groups (–COOH, $–COOCH_3$), and may be assigned to carboxylic acids or their esters [24]. Asymmetric and symmetric stretching vibrations of ionic carboxylic groups ($–COO^-$) appeared, respectively, at 1,641 and 1,423 cm^{-1}. The band at 1,363 cm^{-1} may be assigned to symmetric stretching of $–COO^-$ of pectin [23], the aliphatic acids group vibration at 1,244 cm^{-1} to deformation vibration of C=O and stretching formation of –O–H of carboxylic acids and phenols, and at 1,051 cm^{-1} can be assigned to stretching vibration of C–OH of alcoholic groups and carboxylic acids [25].

It is clear from the FTIR spectrum of OPW that carboxyl and hydroxyl groups were present in abundance. These groups may function as proton donors; hence, deprotonated hydroxyl and carboxyl groups may be involved in coordination with dyes [26]. The FTIR spectrum of TB−OPW showed that the bands expected at 3,419, 1,745, 1,620, 1,423, 1,363, 1,244, and 1,051 cm^{-1} had shifted, respectively, to 3,424, 1,739, 1,641, 1,435, 1,382, 1,240, and 1,051 cm^{-1} due to dye sorption (Fig. 4). These shifts may be attributed to the changes in counter ions associated with carboxylate and hydyroxylate anions, suggesting that acidic groups, carboxyl, and hydroxyl are predominant contributors in dye uptake [27].

3.2. Effect of pH

The pH of dye solution is an important factor in the adsorption process, as it affects the surface charge of the sorbent material and degree of ionization states of functional groups, such as carboxyl and hydroxyl on pectin and cellulose rich sorbents. In order to establish the effect of pH on the adsorption of TB, the batch equilibrium studies at different pH values were carried out in the range of 2.7–10 (Fig. 5(a)). The low dye sorption at pH 2.7 may be explained on the basis of active sites protonation, resulting in H^+ and cationic dye competition to occupy the binding sites [11]. A continuous increase in the sorption capacity of OPW occurred in the pH range of 2.7−3.6 (60% at pH 3.5). This increase in dye removal, as pH increased, can be explained in terms of PZC of the adsorbent (PZC = 3.6). At pH < PZC, the surface of the adsorbent is positively charged. Thus, a decrease in the removal of dye is apparently due to the higher concentration of H^+ ions in the reaction mixture that are competing with the positively charged cations dyes for adsorption sites of OPW [28]. At pH > PZC, the adsorbent is negatively charged and the adsorbate are positively charged. Such a situation enhanced the electrostatic

Table 2
FTIR spectral characteristic of OPW before and after adsorption

Frequency (cm^{-1})			Assignment
Before adsorption	After adsorption TB	Differences	
3,419	3,418	−1	Bonded −OH groups
2,926	2,924	−2	C–H groups
1,745	1,739	−6	C=O stretching
1,620	1,641	+21	COO^- groups
1,423	1,435	+12	COO^- group
1,363	1,382	−19	COO^-
1,244	1,240	+4	C–O–C stretching
1,051	1,051	0	C–O−H stretching
1,029	1,028	−1	C–C groups

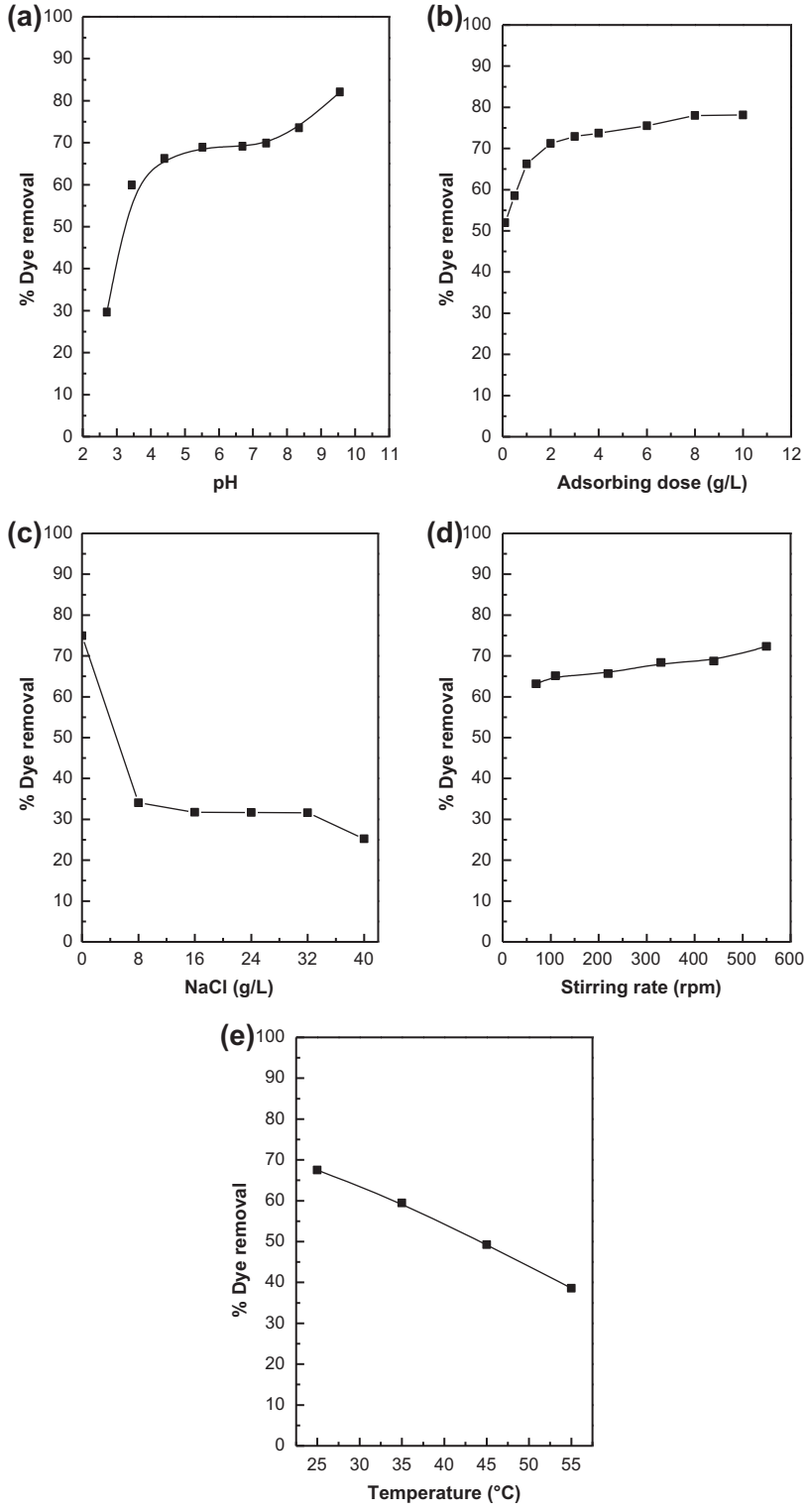

Fig. 5. Effect of (a) solution pH, (b) stirring rate, (c) NaCl, (d) adsorbent dosage, and (e) temperature adsorption of TB on OPW.

attraction between the cationic dye and the negatively charged adsorbent surface [28]. Similar observations have been reported by other authors [29,30]. The following reactions were expected to occur at the solid/liquid interface:

$$OPW + H^+ \rightarrow (OPW)H^+$$

$$OPW + H^+ + TB^+ \rightarrow (OPW)H^+\ TB^+$$

(electrostatic repulsion in acid medium)

$$OPW + OH^- \rightarrow (OPW)\ OH^-$$

$$OPW + OH^- + TB^+ \rightarrow (OPW)\ OH^-TB^+$$

(electrostatic interaction in basic medium)

3.3. Effect of adsorbent dosage

The adsorption of TB onto OPW was studied at different adsorbent dosages (0.1−10 g L^{-1}) of dye solution keeping constant value of other variables; dye concentration (20 mg L^{-1}), stirring speed (220 rpm), pH (6.0), and contact time (30 min). As seen in Fig. 5(b), the percentage dye removal increased from 51.9 to 72.9% for an increase in OPW dose from 0.1 to 3 g L^{-1} and then a slight increase was observed above 3 g L^{-1}. The increase in the percentage of dye removal with adsorbent dosage could be attributed to an increase in the adsorbent surface area, augmenting the number of adsorption sites available for adsorption. The insignificant increase in uptake of dye at OPW dose higher than 3 g L^{-1} may be attributed to the saturation of adsorption sites due to particulate interaction such as aggregation [31]. Based on the obtained results, the 3 g L^{-1} of OPW was selected for further studies.

3.4. Effect of contact time and initial concentration

Fig. 6 represents the adsorption capacity versus the adsorption time at various initial TB concentrations at 25°C. The amount of dye adsorbed (mg g^{-1}) increased with increase in contact time and reached equilibrium after 10 min for the initial dye concentrations ranged from 20 to 160 mg L^{-1}. The equilibrium time is independent of initial dye concentration. As shown in the figure, the uptake of TB as a function of contact time occurs in two phases. The rapid phase (<10 min) is probably due to the abundant availability of active sites on the adsorbent, whereas with the gradual occupancy of the sites, sorption becomes less efficient during the slower phase [32].

3.5. Effect of ionic strength

The effect of salt concentration on the biosorption of TB onto OPW was tested by the addition of different amounts of NaCl (0–40 g L^{-1}) to initial dye solution of 20 mg L^{-1}. As seen in Fig. 5(c), the removal percentage of dye decreases significantly with the increase in the salt concentration. This behavior could be attributed to the competition between cationic dye TB and Na^+ ion for the active sorption sites [33].

3.6. Effect of stirring rate

The effect of stirring rate was studied by varying the stirring speed between 50 and 550 rpm at constant dye concentration (20 mg L^{-1}) and contact time of 30 min. As shown in Fig. 5(d), the sorption of TB on OPW increases slightly with the increase in stirring rate. This is due to the decrease in the thickness of the diffusion layer around the adsorbent surface. Similar results were reported for cationic dyes [34].

3.7. Effect of temperature

The temperature dependence of TB sorption onto OPW was studied with constant initial concentration of 20 mg L^{-1} at 220 rpm and pH 6. The effect of temperature on the sorption of TB by OPW is shown in Fig. 5(e). The removal percentage of dye decreases from 67.6 to 38.5%, when the solution temperature increases from 25 to 55°C. Since the adsorption decreases, when temperature increases, the system is

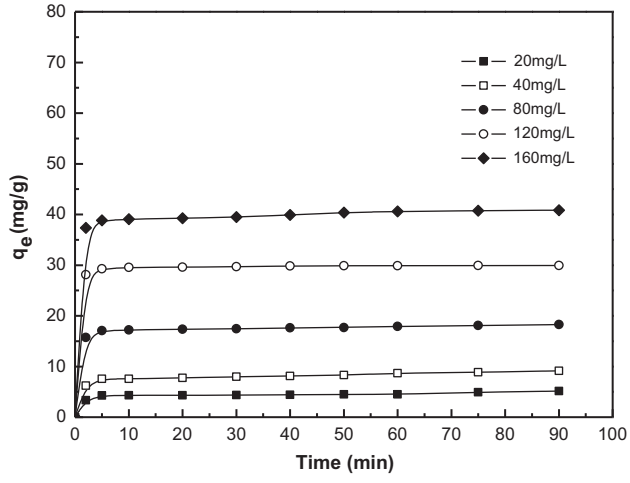

Fig. 6. Effect of initial concentration and contact time on the adsorption of TB (C_0 = 20−160 mg L^{-1}, OPW dosage = 0.3 g, temperature = 25°C, t = 90 min, rpm = 220, pH 6).

considered to be exothermic. The decrease in the adsorption capacity with an increase in temperature is mainly due to the weakening of the interaction forces between the actives sites on the sorbent and the cationic dye and also between adjacent dye molecules on the adsorbed phase [35].

3.8. Adsorption isotherms model

The isotherm model is of importance to optimize the design of an adsorption system to remove the dye. In this study, three isotherms, Langmuir [36], Freundlich [37], and Temkin [38], which are displayed in Table 3, were applied to fit the data of dye adsorption onto OPW. The essential characteristics of the Langmuir isotherm can be expressed by a dimensionless equilibrium parameter (R_L), which is defined by:

$$R_L = \frac{1}{(1 + bC_0)} \tag{3}$$

where b is the Langmuir constant and C_0 (mg L^{-1}) is the highest dye concentration. The value of R_L indicates the type of the isotherm to be either unfavorable ($R_L \geq 1$), linear ($R_L = 1$), favorable ($0 \leq R_L \leq 1$), or irreversible ($R_L = 0$). The values of R_L were found to be 0.871−0.130. These results confirm that the OPW is favorable for the adsorption of TB dye under the experimental conditions used.

Table 4 summarizes the results of the isotherm constants for the three different equilibrium isotherms tested. On the basis of the correlation coefficients (R^2), Langmuir isotherm seemed to represent the equilibrium adsorption data which better fit ($R^2 = 0.987$) as compared to other models (Fig. 7). According to Langmuir model, the adsorption process followed a homogeneous and monolayer mechanism and the maximum monolayer adsorption was 313.4 mg g^{-1}. Table 5 compares the adsorption capacity q_m of different types of adsorbent used for the removal of basic dyes. The value of q_m in this study is larger than those in most of previous works. This suggests that TB could be easily adsorbed on OPW.

3.9. Adsorption kinetics

The adsorption kinetics of TB on the OPW was analyzed using pseudo-first-order and pseudo-second-order kinetic models (Table 6) [42]. The plot of log (q_e–q_t) versus t (Fig. 8) should give a linear relationship from which k_1 and q_e can be determined from the slope and intercept of the plot, respectively, and the plot of t/q_t versus t (Fig. 9) yields very good straight lines for different initial dye concentrations.

The results of fitting experimental data with the pseudo-first-order and pseudo-second-order models for adsorption of dye on OPW are represented in Table 7. As can be seen, the correlation coefficients (R^2) are 0.99 for pseudo-second-order model and less than 0.79 for pseudo-first-order model indicating a better fit with the pseudo-second-order model. The calculated q_e values also agree very well with the experimental data. These results indicate that the adsorption system studied belongs to the second-order kinetic model.

3.10. Thermodynamic parameters

The increase in adsorption with a rise in temperature reveals an endothermic process which can be explained thermodynamically by evaluating parameters such as change in free energy (ΔG°), enthalpy (ΔH°), and entropy (ΔS°). These parameters were calculated using the following equations:

$$\Delta G^\circ = -RT \ln(K_0) \tag{4}$$

$$\ln K_0 = -\frac{\Delta G^\circ}{RT} = \frac{-\Delta H^\circ}{RT} + \frac{\Delta S^\circ}{RT} \tag{5}$$

Table 3
Langmuir, Freundlich, and Temkin isotherms and their non-linear forms

Isotherms	Langmuir	Freundlich	Temkin
Isotherm theory	Monolayer adsorption on homogeneous surface; surface has uniform energy	The adsorption has heterogeneous system; multi-site adsorption	Binding energy was distributed uniformly to the maximum value
Linear form	$\frac{C_e}{q_e} = \frac{1}{q_{max}\, b} + \frac{C_e}{q_{max}}$	$\ln q_e = \ln K_F + \frac{1}{n} \ln C_e$	$q_e = B \ln A + B \ln C_e$
Parameters	b (mg L^{-1}), q_{max} (mg g^{-1})	K_F (mg g^{-1} (L mg^{-1}), n	A(L g^{-1}), B,

Table 4
Constants of adsorption isotherms of TB on OPW

Dye	Langmuir			Freundlich			Temkin		
	q_{max} (mg g^{-1})	b (L mg^{-1})	R^2	K_F	n	R^2	A	B	R^2
TB	313.4	0.0074	0.987	3.273	1.27	0.973	0.161	49.45	0.873

Table 5
Comparison of the maximum adsorption of dyes with various adsorbents

Adsorbents	Dyes	Sorption capacity, q_m (mg g^{-1})	References
Garlic peel	Methylene blue	82.64	[9]
Grapefruit peel	Crystal violet	249.68	[10]
Orange waste	Reactive navy blue	9.21	[12]
Wood apple shell	Methylene blue	95.2	[11]
	Crystal violet	129.8	[11]
Rice husk	Methylene blue	40.50	[39]
Treated ginger waste	Crystal violet	64.9	[40]
Gypsum	Toluidine blue	28	[41]
Orange peel waste	Toluidine blue	313.4	This work

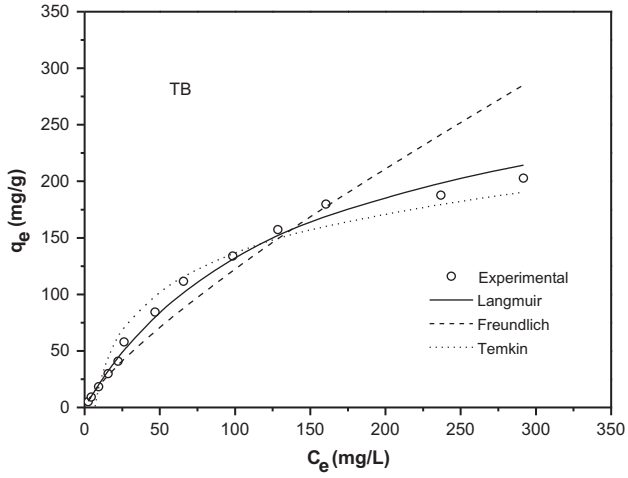

Fig. 7. Isotherm of TB adsorption on OPW.

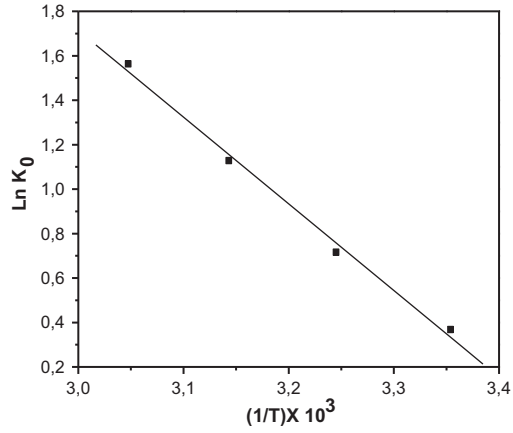

Fig. 8. First-order plot of adsorption of TB on OPW at different dye concentrations.

Table 6
Equations of models

Model	Equation form
Pseudo-first-order model	$\log(q_e - q_t) = \log(q_e) - (\frac{k_1}{2.303})\,t$
Pseudo-second-order model	$\frac{t}{q_t} = \frac{1}{k_2 q_e^2} + \frac{t}{q_e}$

where $K_0 = C_e/q_{max}$, the equilibrium constant of adsorption process (L mg^{-1}). R and T are the gas constant and the absolute temperature, respectively. The plot of Ln K_0 as a function of $1/T$ (Fig. 10) yields a straight line ($R^2 = 0.997$) for TB from which ΔH° and ΔS° were calculated from the slope and intercept, respectively.

The thermodynamic parameters obtained at various temperatures (298, 308, 318, and 328 K) are presented in Table 8. The negative values of ΔG° showed that the adsorption of TB on OPW was of spontaneous

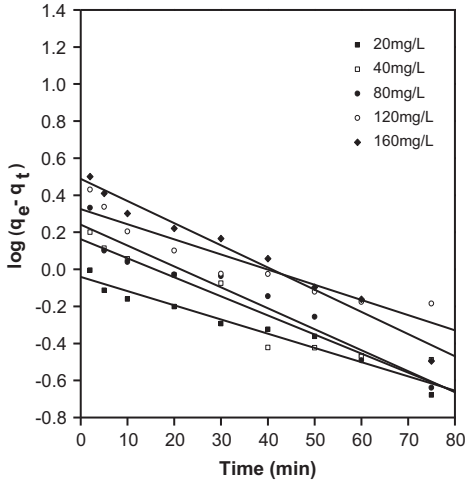

Fig. 9. Second-order plot of adsorption of TB on OPW at different dye concentrations.

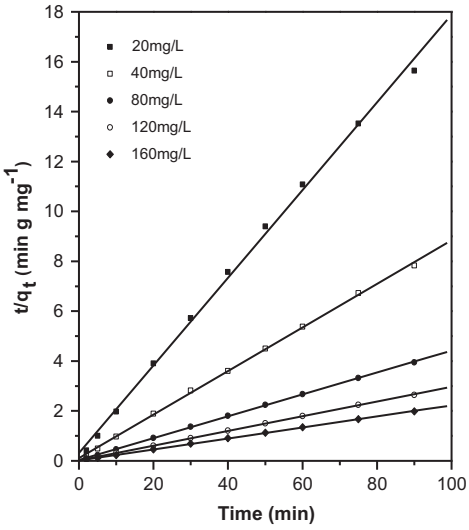

Fig. 10. Thermodynamic parameters of adsorption of TB on OPW.

nature. This was confirmed by the negative value of ΔH° signifying that the adsorption process was exothermic. The positive ΔS° value suggested an increase in the randomness at the solid/solution interface during the adsorption of TB onto OPW [43].

3.11. Biosorption mechanism

OPW is mostly composed of cellulose, pectin, hemicellulose, lignin, chlorophyll pigments, and other low molecular weight hydrocarbons [44]. It is also found to contain carboxyl and hydroxyl functional groups, thus making it a potential adsorbent material for several dyes through ion-exchange and/or complexation mechanism.

To explain the possible mechanism, the PZC played an important role. The surface of waste coffee adsorbent may get mainly positively charged: $OPW \rightarrow OPW^{+}(pH\langle 3.6)$.

Increasing the pH of the solution (pH > 3.6), due to the findings from PZC experiments, the surface of OPW is charged negatively: $OPW \rightarrow OPW^{-}(pH\rangle 3.6)$.

$$OPW - OH(\text{Phenolic groups}) \rightarrow OPW - O^{-}$$

$$OPW - O^{-} + D - Cl \rightarrow OPW - O - D + Cl^{-}$$

In alkaline conditions, where the full deprotonation dominates, the interaction between the adsorbent and dye is completely controlled by electrostatic and coulombic strong forces, between the negatively charged functional groups of OPW (especially the carboxylic groups) and the constant localized positive charge of the cationic dye.

$$OPW - COO^{-} + D^{+} \rightarrow OPW - COO^{-}D^{+}$$

On the basis of the FTIR spectrum and active site analysis, a proposed mechanism for the biosorption of the TB onto OPW is shown in Fig. 11.

Table 7
Kinetic parameters for biosorption of TB on OPW

Dye	C_0 (mg L^{-1})	Pseudo-first-order kinetics			Pseudo-second-order kinetics		
		q_e (mg g^{-1})	k_1 (min^{-1})	R^2	q_e (mg g^{-1})	k_2 (g mg min^{-1})	R^2
TB	20	1.782	0.0176	0.627	5.690	0.0994	0.998
	40	3.288	0.0236	0.796	11.448	0.0730	0.999
	80	3.090	0.0260	0.676	22.779	0.0628	0.999
	120	2.208	0.0188	0.723	33.863	0.0531	0.999
	160	6.208	0.0275	0.773	45.248	0.0369	0.999

Table 8
Thermodynamic parameters for the adsorption of TB onto OPW

Dye	$-\Delta H^\circ$ (kJ mol^{-1})	ΔS° (kJ K.mol^{-1})	$-\Delta G^\circ$ (kJ mol^{-1})			
			298 K	308 K	318 K	328 K
TB	32.443	0.111	65.710	66.826	67.942	69.058

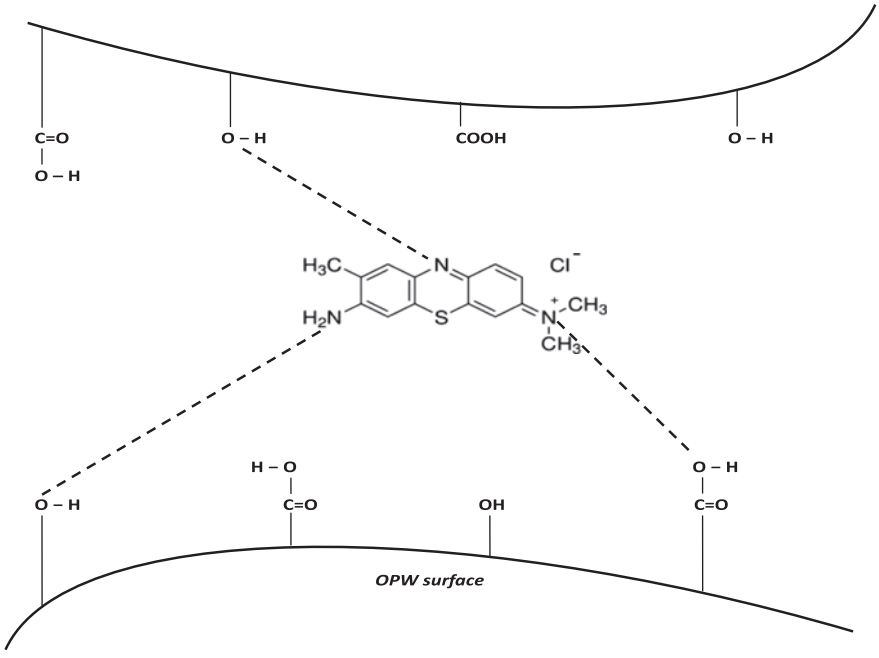

Fig. 11. Proposed mechanism of adsorption of TB on OPW.

4. Conclusion

The adsorption potential of untreated OPW for the removal of TB from aqueous solution was investigated under varying conditions of initial concentration, adsorbent dosage, pH, and temperature. Equilibrium data demonstrated favorable adsorption and were better described by Langmuir model in comparison to both Freundlich and Tempkin models. The maximum value of uptake capacity obtained for the (OPW)/TB system (=313.4 mg g^{-1}) was higher than the values encountered in the literature for other untreated agricultural by-products. The adsorption is rapid; the equilibrium is obtained within 10 min, and favorable according to thermodynamic parameters. Adsorption kinetics was well described by the pseudo-second-order kinetic model. The results obtained in this study indicate that OPW presents great potential as an inexpensive and easily available alternative adsorbent for the removal of TB from aqueous solutions.

Symbols

b — Langmuir's constant related to energy of adsorption, L m g^{-1}
B — constant related to the heat of adsorption, J mol^{-1}
C_0 — initial concentration of dye, mg L^{-1}
C_e — equilibrium concentration of dye, mg L^{-1}
K_L — equilibrium constant at temperature T
k_1 — rate constant of pseudo-first-order adsorption, L min^{-1}
k_2 — rate constant of pseudo-second-order adsorption, g/mg min
K_F — Freundlich constant
n — Freundlich constant
q_e — adsorption capacity at equilibrium, mg g^{-1}
q_t — adsorption capacity at time t, mg g^{-1}
q_{max} — Langmuir's constant related to capacity of adsorption, mg g^{-1}
R — ideal gas constant, kJ mol K^{-1}
R^2 — regression coefficient
R_L — equilibrium parameter, dimensionless

T — time, min
T — absolute temperature, K
V — volume of dye solution, L
W — weight of adsorbent, g
ΔG° — standard free energy change, kJ mol^{-1}
ΔH° — standard enthalpy change, kJ mol^{-1}
ΔS° — standard entropy change, kJ $K\ mol^{-1}$

References

[1] I.M. Banat, P. Nigam, D. Singh, R. Marchant, Microbial decolorization of textile-dye-containing effluents: A review, Bioresour. Technol. 58 (1996) 217–227.
[2] O.J. Hao, H. Kim, P.C. Chiang, Decolorization of wastewater, Crit. Rev. Env. Sci. Technol. 30 (2000) 449–505.
[3] S. Chinwetkitvanich, M. Tuntoolvest, T. Panswad, Anaerobic decolorization of reactive dye bath effluents by a two-stage UASB system with tapioca as a co-substrate, Water Res. 34 (2000) 2223–2232.
[4] J. Panswed, S. Wongchaisuwan, Mechanism of dye wastewater color removal by magnesium carbonate-hydrated basic, Water Sci. Technol. 18 (1986) 139–144.
[5] P.K. Malik, S.K. Saha, Oxidation of direct dyes with hydrogen peroxide using ferrous ion as catalyst, Sep. Purif. Technol. 31 (2003) 241–250.
[6] G. Ciardelli, L. Corsi, M. Marucci, Membrane separation for wastewater reuse in the textile industry, Resour. Conserv. Recycl. 31 (2000) 189–197.
[7] A. Bhatnagar, M. Sillanpaa, Utilization of agro-industrial and municipal waste materials as potential adsorbents for water treatment: A review, Chem. Eng. J. 157 (2010) 277–296.
[8] A. Demirbas, Agricultural based activated carbons for the removal of dyes from aqueous solutions: A review, J. Hazard. Mater. 167 (2009) 1–9.
[9] B.H. Hameed, A.A. Ahmad, Batch adsorption of methylene blue from aqueous solution by garlic peel, an agricultural waste biomass, J. Hazard. Mater. 164 (2009) 870–875.
[10] A. Saeeda, M. Sharif, M. Iqbal, Application potential of grapefruit peel as dye sorbent: Kinetics, equilibrium and mechanism of crystal violet adsorption, J. Hazard. Mater. 179 (2010) 564–572.
[11] S. Jain, R.V. Jayaram, Removal of basic dyes from aqueous solution by low-cost adsorbent: Wood apple shell (*Feronia acidissima*), Desalination 250 (2010) 921–927.
[12] S. Irem, Q.M. Khan, E. Islam, A.J. Hashmat, M.A. ul Haq, M. Afzal, T. Mustafa, Enhanced removal of reactive navy blue dye using powdered orange waste, Eco. Eng. 58 (2013) 399−405.
[13] A.K. Bejar, N.B. Mihoubi, N. Kechaou, Moisture sorption isotherms—Experimental and mathematical investigations of orange (*Citrus sinensis*) peel and leaves, Food Chem. 132 (2012) 1728–1735.
[14] M.R. Wilkins, W. Widmer, K. Grohmann, R.G. Cameron, Hydrolysis of grapefruit peel waste with cellulase and pectinase enzymes, Bioresour. Technol. 98 (2007) 1596–1601.
[15] S.V. Ting, E.J. Deszyck, The carbohydrates in the peel of oranges and grapefruit, J. Food Sci. 26 (1961) 146–152.
[16] R.S. Blackburn, Natural polysaccharides and their interactions with dye molecules: Applications in effluent treatment, Environ. Sci. Technol. 38 (2004) 4905–4909.
[17] H.P. Boehm, Some aspects of the surface chemistry of carbon blacks and other carbons, Carbon 32 (1994) 759–769.
[18] I.D. Mall, V.C. Srivastava, G.V.A. Kumar, I.M. Mishra, Characterization and utilization of mesoporous fertilizer plant waste carbon for adsorptive removal of dyes from aqueous solution, Colloids Surf. A 278 (2006) 175–187.
[19] M. Thirumavalavan, Y.L. Lai, L.C. Lin, J.F. Lee, Cellulose-based native and surface modified fruit peels for the adsorption of heavy metal ions from aqueous solution: Langmuir adsorption isotherms, J. Chem. Eng. Data 55 (2009) 1186–1192.
[20] M.L. González-Martín, C. Valenzuela-Calahorro, V. Gómez-Serrano, Characterization study of carbonaceous materials. Calorimetric heat of adsorption of p-nitrophenol, Langmuir 10 (1994) 844–854.
[21] D. Mohan, C.U. Pittman Jr, M. Bricka, F. Smith, B. Yancey, J. Mohammad, P.H. Steele, M.F. Alexandre-Franco, V. Gómez-Serrano, H. Gong, Sorption of arsenic, cadmium, and lead by chars produced from fast pyrolysis of wood and bark during bio-oil production, J. Colloid Interface Sci. 310 (2007) 57–73.
[22] R. Gnanasambandam, A. Protor, Determination of pectin degree of esterification by diffuse reflectance Fourier transform infrared spectroscopy, Food Chem. 68 (2000) 327–332.
[23] F.T. Li, H. Yang, Y. Zhao, R. Xu, Novel modified pectin for heavy metal adsorption, Chin. Chem. Lett. 18 (2007) 325–328.
[24] N.V. Farinella, G.D. Matos, M.A.Z. Arruda, Grape bagasse as a potential biosorbent of metals in effluent treatments, Bioresour. Technol. 98 (2007) 1940–1946.
[25] G. Guibaud, N. Tixier, A. Bouju, M. Baudu, Relationship between extracellular polymer's composition and its ability to complex Cd, Cu and Pb, Chemosphere 52 (2003) 1701–1710.
[26] M. Iqbal, A. Saeeda, S.I. Zafar, FTIR spectrophotometry, kinetics and adsorption isotherms modeling, ion exchange, and EDX analysis for understanding the mechanism of Cd^{2+} and Pb^{2+} removal by mango peel waste, J. Hazard. Mater. 164 (2009) 161–171.
[27] V. Ponnusami, V. Gunasekar, S.N. Srivastava, Kinetics of methylene blue removal from aqueous solution using gulmohar (*Delonix regia*) plant leaf powder: Multivariate regression analysis, J. Hazard. Mater. 169 (2009) 119–127.
[28] R. Ahmad, Studies on adsorption of crystal violet dye from aqueous solution onto coniferous pinus bark powder (CPBP), J. Hazard. Mater. 171 (2009) 767–773.
[29] M. Ramakrishnan, S. Nagarajan, Utilization of waste biomass for the removal of basic dye from water, World Appl. Sci. J. 5 (2009) 114–121.
[30] P. Monash, G. Pugazhenthi, Adsorption of crystal violet dye from aqueous solution using mesoporous materials synthesized at room temperature, Adsorption 15 (2009) 390–405.
[31] S. Chakraborty, S. Chowdhury, P.D. Saha, Adsorption of crystal violet from aqueous solution onto NaOH-modified rice husk, Carbohydr. Polym. 86 (2011) 1533–1541.

[32] M. Iqbal, A. Saeed, Biosorption of reactive dye by loofa sponge-immobilized fungal biomass of *Phanerochaete chrysosporium*, Process Biochem. 42 (2007) 1160–1164.
[33] R. Gonga, Y. Dingb, M. Lic, C. Yanga, H. Liua, Y. Suna, Utilization of powdered peanut hull as biosorbent for removal of anionic dyes from aqueous solution, Dyes Pigm. 64 (2005) 187–192.
[34] V.K. Garg, M. Amita, R. Kumar, R. Gupta, Basic dye (methylene blue) removal from simulated wastewater by adsorption using Indian Rosewood sawdust: A timber industry waste, Dyes Pigm. 63 (2004) 243–250.
[35] A.E. Ofomaja, Y.S. Ho, Equilibrium sorption of anionic dye from aqueous solution by palm kernel fibre as sorbent, Dyes Pigm. 74 (2007) 60–66.
[36] I. Langmuir, The constitution and fundamental properties of solids and liquids, J. Am. Chem. Soc. 38(11) (1916) 2221–2295.
[37] H.M.F. Freundlich, Over the adsorption in solution, J. Phys. Chem. 57 (1906) 385–471.
[38] M.J. Temkin, V. Pyzhev, Recent modifications to Langmuir isotherms, Acta Physiochim. USSR 12 (1940) 217–222.
[39] V. Vadivelan, K. Kumar, Equilibrium, kinetics, mechanism, and process design for the sorption of methylene blue onto rice husk, J. Colloid Inter. Sci. 286 (2005) 90–100.
[40] R. Kumar, R. Ahmad, Biosorption of hazardous crystal violet dye from aqueous solution onto treated ginger waste (TGW), Desalination 265 (2011) 112–118.
[41] M.A. Rauf, S.M. Qadri, S. Ashraf, K.M. Al-Mansoori, Adsorption studies of Toluidine Blue from aqueous solutions onto gypsum, Chem. Eng. J. 150 (2009) 90–95
[42] D.M. Ruthven, Principles of Adsorption and Adsorption Process, Wiley, New York, NY, 1984.
[43] C. Varlikli, V. Bekiari, M. Kus, N. Boduroglu, I. Oner, P. Lianos, G. Lyberatos, S. Icli, Adsorption of dyes on Sahara desert sand, J. Hazard. Mater. 170 (2009) 27–34.
[44] R.P. Dhakal, K.N. Ghimire, K. Inoue, Adsorptive separation of heavy metals from an aquatic environment using orange waste, Hydrometallurgy 79 (2005) 182–190.